ISSN: 2277-9655
Scientific Journal Impact Factor: 3.449
(ISRA), Impact Factor: 2.114

IJESRT

INTERNATIONAL JOURNAL OF ENGINEERING SCIENCES & RESEARCH TECHNOLOGY

ANALYSIS OF HELICAL BAFFLE HEAT EXCHANGER FOR OPTIMUM HELIX ANGLE THROUGH NUMERICAL SIMULATIONS

Roktutpal Borah[1], R.K Chitharthan[2]

[12] Department of mechanical engineering, Hindustan University, Chennai, India

ABSTRACT

Heat exchangers are very important heat & mass exchange apparatus in many industries like electric power generation, chemical industries, oil refining, etc. The most common heat exchangers used are shell-&-tube heat exchangers (STHXs). Among different kinds of baffles used in STHX, segmental baffles are most commonly used in conventional STHXs to support tubes & change fluid flow direction. But, conventional heat exchangers with segmental baffles in shell-side have some drawbacks like higher pressure drop. Such drawbacks can be reduced by using helical baffle in the shell side of STHX i.e. helixchanger. In a helixchanger the pressure drop varies with the variation of helix angle, thus the performance. This paper is based on the prediction of optimum helix angle based on the parameters like pressure drop variation and heat transfer coefficient, by carrying out 3D simulation for different helix angles (30^0, 35^0, 40^0, 45^0, 50^0). The modeling was done by using CATIA V5 r18 and the analysis was carried out by using cfd tool ANSYS 14.5.

KEYWORDS: helical baffles, helix angle, pressure drop, heat transfer coefficient, ANSYS 14.5.

INTRODUCTION

The shell and tube heat exchanger is the heat transfer equipment most widely used in the current industrial production. More than 35–40% of heat exchangers are of the shell-and-tube type due to their robust geometry construction, easy maintenance and possible upgrades [1]. Compared with other types, its main advantages are the large heat transfer area in the unit volume and good heat transfer effect. It is widely used in many industrial areas, such as power plant, chemical engineering, petroleum refining, and food processing, etc, as simple structure, wide range of materials required in manufacturing, and greater operation flexibility. The shape and arrangement of baffles are of essential importance for the performance of heat exchangers. The segmental baffle is most common, which forces the shell-side fluid going through in a zigzag manner, to increase the speed of shell fluid and intensify the turbulent level. Hence the improvement of heat transfers with a large pressure drop penalty. This type of heat exchanger has been well-developed [2-5], and probably is still the most commonly used type of the STHX. Due to the flow dead zone between segmental baffles and the shell fluid undergoes repeated movement of cross streams, resulting in the reduction of driving force of heat transfer. For obtaining higher heat transfer performance, only the plate spacing is reduced, and causes a higher flow resistance at the cost of higher energy consumption. The heat exchanger with helical baffles becomes an ideal alternative. This type of baffle was first developed by Lutcha and Nemcansky [6]. It uses the continuous helical backing plate in support of heat exchange tube to make the shell medium do the inclined forward movement along the spiral channel from the shell entrance. The Helical Baffle heat Exchanger removes many of the deficiencies of Segmental Baffle Heat Exchanger. For example, in [7] a comprehensive comparison is provided from experimental data between the STHXsHB and STHXsSB. It is concluded that based on the same pumping power the STHXsHB can have appreciably better performance than that of STHXsSB. M.R. Jafari Nasr et al [8] found that velocity distribution of flow in shell side in helical baffle system is more uniform and homogenous than segmental baffle system. This leads to less fouling rate and also less erosion occurrence inside the shell. Also Helical baffles provide smooth behavior of the fluid flow in the shell side which leads to lower pressure drop [9] as there is no dead zone and has stable thermal resistance. Wen-Quan Tao et al [10] compared numerically simulated data and experimental data and found the maximum differences between

ISSN: 2277-9655
Scientific Journal Impact Factor: 3.449
(ISRA), Impact Factor: 2.114

numerical results and experimental data are around 25% for pressure drop and 15% for Nu number. Qiuwang Wang et al [11] in his paper found that under the same mass flow rate M and overall heat transfer rate Q_m, the average overall pressure drop Δp_m of the CMSP-STHX is lower than that of conventional SG-STHX by 13% on average. Under the same overall pressure drop Δp_m in the shell side, the overall heat transfer rate Q_m of the CMSP-STHX is nearly 5.6% higher than that of SG-STHX and the mass flow rate in the CMSP-STHX is about 6.6% higher than that in the SG-STHX

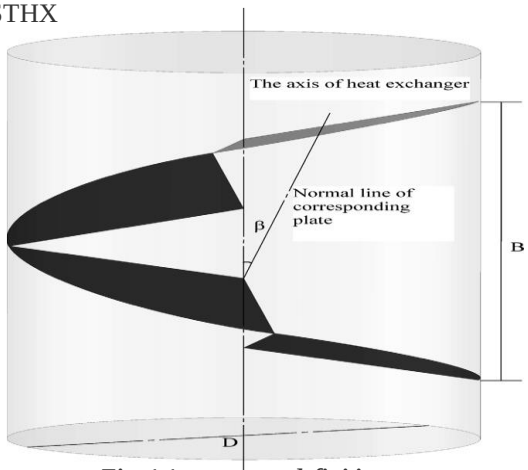

Fig. 1.1 parameter definition

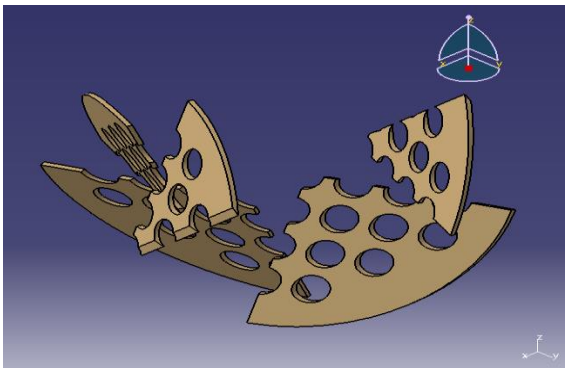

Fig. 1.2 isometric view of non-continuous helical baffle

.

Nomenclature

A_o = heat exchange area based on the outer diameter of tube, m^2
B = baffle spacing for segmental baffles or helical pitch for helical baffles, mm
c_p = specific heat, J/(kg K)
D_i = inside diameter of shell, mm
D_o = outside diameter of shell, mm
D_1 = tube bundle-circumscribed circle diameter, mm
De= equivalent diameter, mm
d_i = tube inner diameter, mm
d_o = outer diameter of tube, mm
Gs= mass velocity of shell side, $kg/m^2.s$
h = heat transfer coefficient, W/ (m^2 K)
k = turbulent kinetic energy
l = effective length of tube, mm
M = mass flow rate, kg/s
N_t = number of tubes
Δp = shell-side pressure drop, kPa
q_s = volume flow rate, m3 h_1
Re = Reynolds number
A_s = cross-flow area at the shell centerline, mm2
Δt_m = logarithmic mean temperature difference, K
t = temperature, K
t_p = tube pitch, mm
u = fluid velocity in the shell side, m s_1
β = helix angle
Φ = heat exchange quantity, W
κ = thermal conductivity, W/ (m K)
μ = dynamic viscosity of fluid, kg/ms
ρ = density of fluid, kg/m^3

Subscripts

in = inlet
out = outlet
s = shell side
t = tube side
w = wall

HEAT EXCHANGER MODEL FOR SIMULATION

Computational model

The computational model for this paper is adopted from an experimentally tested STHXHB [7]. The geometry parameters of STHXHB for the entire helix angle (30^0, 35^0, 40^0, 45^0, 50^0) analyzed are listed in the table 2.1 below. The whole computation domain is bounded by the inner side of the shell and everything in the shell contained in the domain. The model has 24 nos. of baffles with total tube number of 37.

Table 2.1 geometry parameters

Parameters	Dimensions and description				
Do (mm)	223	223	223	223	223
Di (mm)	211	211	211	211	211
No. of tubes	37	37	37	37	37
tube pitch t_p (mm)	25	25	25	25	25
length l (mm)	1195	1397	1703	2034	2367
Baffle pitch (mm)	168	200	250	303	356
Baffle thickness mm	3	3	3	3	3
No. of Baffles	24	24	24	24	24
Helix angle	30^0	35^0	40^0	45^0	50^0

Assumptions to simplify numerical simulation:

1. The shell side fluid is constant thermal properties

ISSN: 2277-9655
Scientific Journal Impact Factor: 3.449
(ISRA), Impact Factor: 2.114

2. The fluid flow and heat transfer processes are turbulent and in steady state
3. The leak flows between tube and baffle and that between baffles and shell are neglected
4. The natural convection induced by the fluid density variation is neglected
5. The tube wall temperature kept constant
6. The heat exchanger is well insulated hence the heat loss to the environment is totally neglected

Navier-Stokes Equation:

It is also a fundamental equation used by ANSYS and solves in every mesh cell and the simulation shows the result. The derivation of the Navier Stokes equation begins with an application of second law of Newton i.e. conservation of momentum. In an inertial frame of reference, the general form of the equations of fluid motion is:-

$$\partial_x u + \partial_y v + \partial_z \omega = 0 \quad (1)$$

$$\partial_\tau u + u\partial_x u + v\partial_y u + \omega\partial_z u = -\partial_x p + \frac{1}{Re}[\mu(\partial_x^2 u + \partial_y^2 u + \partial_z^2 u) + \mu\partial_x(\partial_x u + \partial_y v + \partial_z \omega)] \quad (2)$$

$$\partial_\tau v + u\partial_x v + v\partial_y v + \omega\partial_z v = -\partial_y p + \frac{1}{Re}[\mu(\partial_x^2 v + \partial_y^2 v + \partial_z^2 v) + \mu\partial_y(\partial_x u + \partial_y v + \partial_z \omega)] \quad (3)$$

$$\partial_\tau \omega + u\partial_x \omega + v\partial_y \omega + \omega\partial_z \omega = -\partial_z p + \frac{1}{Re}[\mu(\partial_x^2 \omega + \partial_y^2 \omega + \partial_z + \mu\partial_z(\partial_x u + \partial_y v + \partial_z \omega)] \quad (4)$$

$$\partial_\tau T + u\partial_x T + v\partial_y T + \omega\partial_z T = -\frac{1}{RePr}[\partial_x(k\partial_x T) + \partial_y(k\partial_Y T) + \partial_z(k\partial_Z T)] \quad (5)$$

Grid Generation

The 3-D model is discretized in ICEM CFD. Model is discretized with unstructured tetrahedral elements and the region adjacent to the tubes is meshed much finer by decreasing the element size in the tube surface which allows capturing the boundary layer gradient accurately.

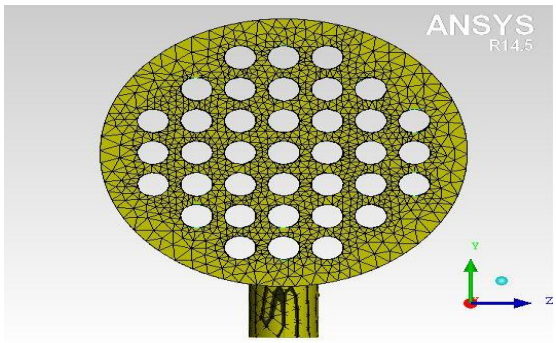

Fig. 2.2 front view of grid heat exchanger head

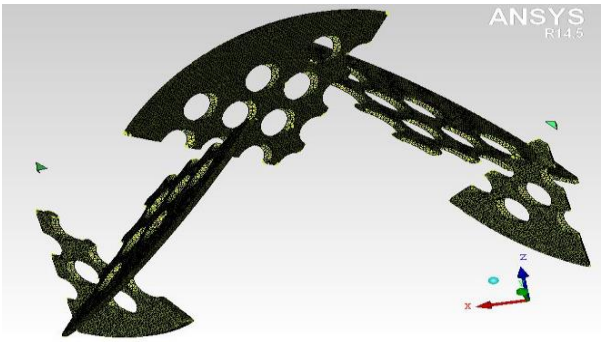

Fig. 2.3 section of grid of baffle

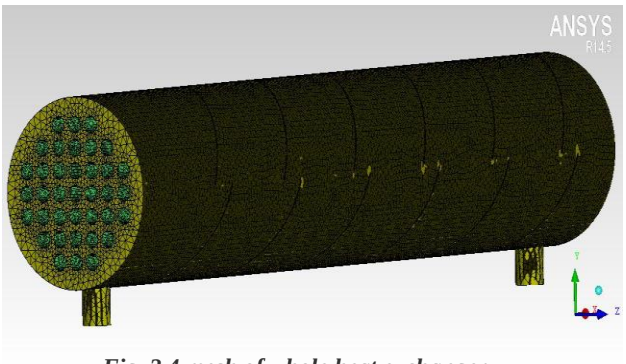

Fig. 2.4 mesh of whole heat exchanger

The total nos. of elements for each model with different helix angles are 2399724, 2782250, 3376962, 2363540, 1976208 respectively. The meshes are checked for minimum required quality

Boundary conditions and problem setup

The boundary conditions are set in ANSYS CFX-pre. First the domains are defined and the inlet outlet locations. Reference pressure is set at 1 atm, the conductive-320 oil is taken as working fluid for shell side. Heat transfer is set as thermal energy and the viscous was set as standard k-e(k-epsilon 2 eqn). The mass-flow-inlet and outflow boundary condition are applied on the inlet with 318.5 K inlet temperature and outlet with relative pressure 0 pa, respectively. The temperature of tube walls are set as 289.4 K, the average wall temperature determined in the experiments. The inner wall of the shell and all solid surfaces set as non-slip. The shell wall of heat exchanger is set as adiabatic. All the solid domains are made of steel. In solver control the advection scheme was set as upwind and turbulence as 1st order. Simulation was carried out in ANSYS CFXv14.5.

Table 2.2 properties of shell fluid conduction oil

ISSN: 2277-9655
Scientific Journal Impact Factor: 3.449
(ISRA), Impact Factor: 2.114

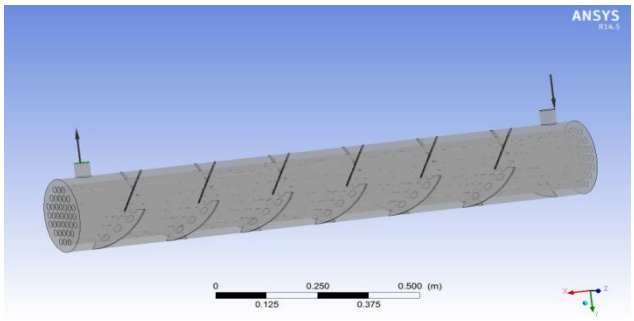

Fig. 2.5 domain of shell fluid

2.5. Formulas used for Data reduction

2.5.1 The shell-side fluid mean velocity

$U = q_s/A_S$

$Gs = m_s/ A_S$

For the noncontinuous helical baffles

$A_S = 0.5B [D_i - D_1 + ((D_1 - d_o)/t_p (t_p - d_o))]$

$B = \sqrt{2}D_i - \tan\beta$ (middle-overlapped helical baffle)

$D_e = 4[p_t^2 - (\pi/4)d_o^2]/ \pi d_o$

The Reynolds number of shell-side fluid:

$Re_s = (Gs \times D_e)/\mu$

2.5.2 Shell-side heat transfer coefficient

Heat exchange rate of shell-side fluid:

$\Phi_s = M_s \times cps (t_s in - t_s out)$

$h_s = \Phi_s/ A_o - \Delta t_m$ [9].

$A_o = N_t \pi d_o l$

$\Delta t_m = \Delta t_{max} - \Delta t_{min}$

$\Delta t_{max} = t_s in - t_w$

$\Delta t_{min} = t_s out - t_w$

COMPUTATIONAL MODEL VALIDATION

The computational model of 40^0 helix angle was first analyzed for different mass flow rate for validation of the computational model used in the project. The experimental data are taken from ref [7]. The corresponding values of shell side heat transfer coefficient of different mass flow rate from the analysis are given in the table 3.1. The maximum deviation of shell side heat transfer coefficient is of 9.83%.

Table 3.1 validation of the computational model

Parameter	Value
Specific heat capacity cp (J/kg K)	2270.1
Dynamic viscosity μ (kg/ms)	0.0095
Density ρ (kg/m3)	826.1
Thermal conductivity k (W/m K)	0.132

volume flow rate (m2/hr)	mass flow rate (kg/s)	shell side heat transfer coefficient experimental ($W/m^2.k$)	shell side heat transfer coefficient analysis ($W/m^2.k$)	Deviation %
7.8	1.789	255	232.162	9.83%
9.6	2.2	278	256.291	8.47%
17.1	3.923	373	357.646	4.29%
18.9	4.337	391	358.773	8.90%

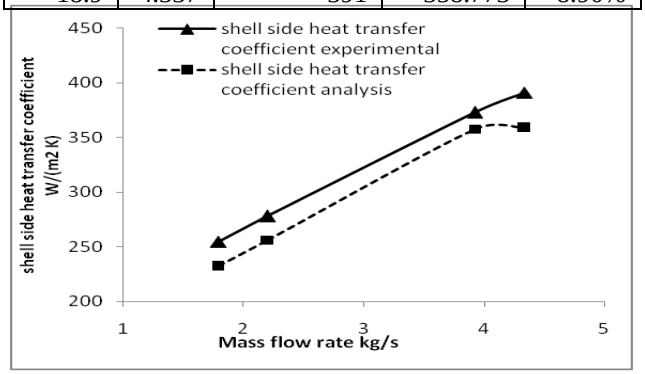

Fig.3.1 Comparison of shell side heat transfer coefficient between experimental results and simulation results

RESULTS AND DISCUSSION

Simulations were made with the models of above mentioned (table 2.1) geometry parameters. Simulation results of different helix angles heat exchanger are showed in the table (4.1-4.4) below

Table 4.1 simulation results at mass flow rate 4.337 kg/s

β	Outlet t (K)	Φ, (W)	h_s ,(W/ (m^2 K))	ΔP (Kpa)	$h_s/\Delta P$ W/ (m^2 Kpa K)
30°	316.442	20261.882	273.574	14.271	19.169
35°	316.061	24012.988	286.613	13.169	21.779
40°	314.779	36634.821	357.851	13	27.527
45°	315.23	32489.898	263.683	12.188	21.634
50°	315.994	24643.095	169.461	12.13	14.005

ISSN: 2277-9655
Scientific Journal Impact Factor: 3.449
(ISRA), Impact Factor: 2.114

Table 4.2 simulation results at mass flow rate 3.923 kg/s

β	Outlet t (K)	Φ, (W)	h_s ,(W/ (m^2 K))	ΔP (Kpa)	h_s/ΔP W/ (m^2 Kpa K)
30°	315.764	13664.185	16.858	3.777	49.468
35°	315.266	16151.307	195.598	3.599	54.338
40°	313.397	25485.504	256.03	3.414	74.993
45°	314.862	18168.972	148.482	3.396	43.722
50°	315.129	16835.515	117.6366	3.351	35.103

Table 4.3 simulation results at mass flow rate 2.2 kg/s

β	Outlet t (K)	Φ, (W)	h_s (W/ (m^2 K))	ΔP (Kpa)	h_s/ΔP W/ (m^2 Kpa K)
30°	316.693	16101.329	216.461	11.801	18.342
35°	316.485	17944.788	212.449	11.252	18.88
40°	314.426	36281.423	357.128	10.7	33.375
45°	316.093	21435.784	171.165	10.62	16.116
50°	316.132	21088.466	144.609	10.302	14.036

Table 4.4 simulation results at mass flow rate 1.789 kg/s

β	Outlet t (K)	Φ, (W)	h_s ,(W/ (m^2 K))	ΔP (Kpa)	h_s/ΔP W/ (m^2 Kpa K)
30°	315.234	13263.908	183.192	2.516	72.788
35°	314.86	14782.8	180.41	2.396	75.276
40°	312.87	22864.606	232.172	2.27	102.234
45°	314.16	17625.646	146.019	2.259	64.638
50°	314.68	15513.818	109.337	2.238	48.839

Pressure variations

In pressure distribution contour across the shell fluid of 40^0 helix angle heat exchanger in fig.4.1 across the baffle wall we can see the pressure decreases gradually from inlet towards outlet. The variation trends of pressure drops with mass flow rate are shown in Fig. 4.2. At the same mass flow rate and shell inner diameter, the pressure drop decreases with the increasing of helix angel.

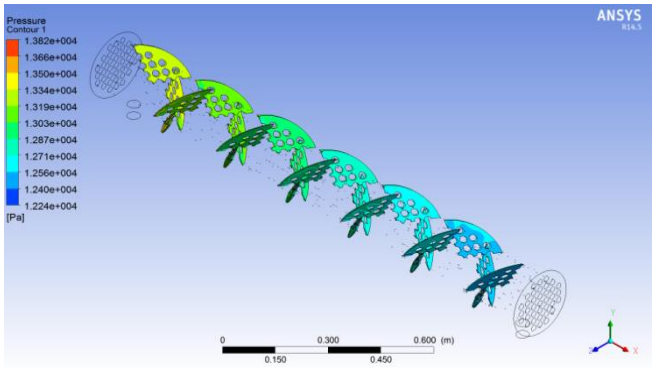

Fig.4.1 Pressure distribution across the shell fluid of 40^0 helix angle heat exchanger

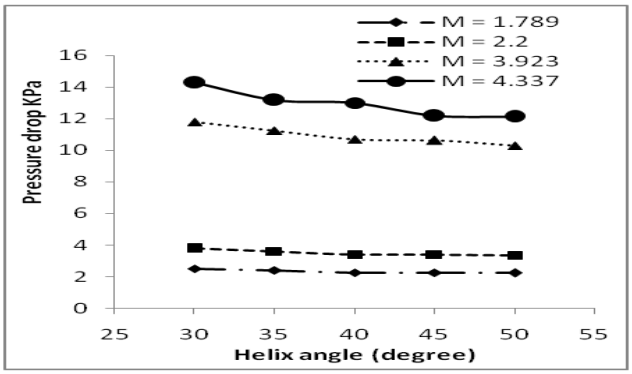

Fig. 4.2 variation of pressure drop in various helix angles

Temperature and shell side heat transfer coefficient variations

In the temperature distribution contour of fluid near the baffle, temperature is lower near the tube wall and gradually increases towards shell inner diameter across the shell fluid fig.4.2 and in the xy plane temperature gradually decreases towards outlet. The outlet temperature, thus heat transfer coefficient varies with change in helix angle, table (4.1-4.4). The variation trends of heat transfer coefficient are shown in Fig. 4.4.

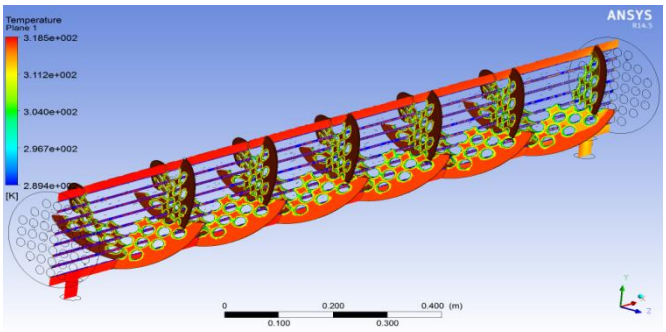

ISSN: 2277-9655
Scientific Journal Impact Factor: 3.449
(ISRA), Impact Factor: 2.114

Fig.4.3 Temperature distribution across the shell fluid of 40^0 helix angle heat exchanger

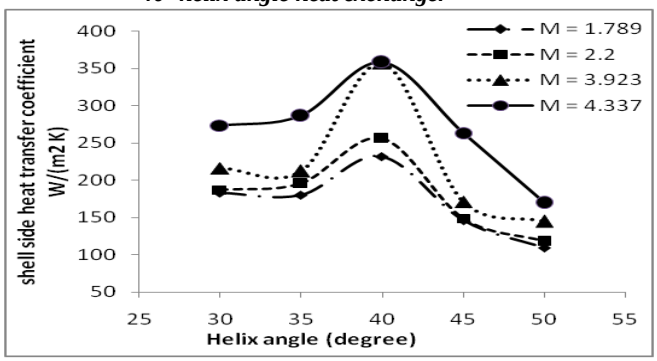

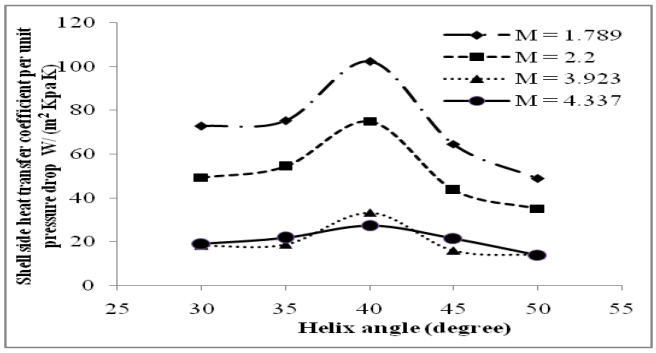

Fig. 4.4 variation of shell side heat transfer coefficients in various helix angels

Fig. 4.5 variation of shell side heat trnsfer coefficient per unit pressure drop in various helix angles

CONCLUSION

An experimentally tested STHXHB model for this paper is adopted. First the model was validated with 40^0 helix angle for different mass flow rate. Then the simulations were carried out for various helix angels (30^0, 35^0, 40^0, 45^0, 50^0). From the simulation results we can gather that:

1. At the same mass flow rate and shell inner diameter, the pressure drop decreases with the increasing of helix angel.
2. The heat transfer coefficient in shell side starts increasing till helix angle 40^0 but starts gradually decreasing after that.
3. In the ratio of shell side heat transfer coefficient per unit pressure drop it can clearly be observed that 40^0 helix angle is the optimum helix angle

REFERENCES

1. B.I. Master,Fouling mitigation using helixchanger heat exchangers, in: Proceedings of the ECI Conference on Heat Exchanger Fouling and Cleaning: Fundamentals and Applications, Santa Fe, NM, May 18–22 2003, pp. 317–322.
2. Bell, K.J., 1981. Delaware method for shell side design. In:Kakac, S ., Bergles, A.E., Mayinger, F.(Eds.), Heat Exchangers-Thermal-Hydraulic Fundamentals and Design. Taylor & Francis, Washington, DC.
3. Bell, K.J., 1986. Delaware method of shell side design. In:Pallen,J.W.(Ed.), Heat Exchanger Source book. Hemisphere, NewYork.
4. Bell, K.J., 1988. Delaware method of shell-side design. In: Shah, R.K., Sunnarao, E.C., Mashelkar, R.A.(Eds.), Heat Transfer Equipment Design. Taylor & Francis, New York.
5. Bell, K.J.,2004. Heat exchanger design for the process industries. ASME Journal of Heat Transfer 126(6), 877–885.
6. Lutcha, J, Nemcansky, J,1990, Performance Improvement of Tubular Heat Exchangers by Helical Baffles, Trans.Inst.Chem.Eng., Part A, 68, pp.263–270.
7. Jian-Fei Zhang, Bin Li, Wen-Jiang Huang, Yong-Gang Lei, Ya-Ling He, Wen- Quan Tao, Experimental performance comparison of shell side heat transfer for shell-and-tube heat exchangers with middle-overlapped helical baffles and segmental baffles, Chem. Eng. Sci. 64 (2009) 1643
8. M.R. Jafari Nasr, Fluid flow analysis and extension of rapid design algorithm for helical baffle heat exchangers, Applied Thermal Engineering 28(2008)1324–1332
9. Sirous Zeyninejad Movassag, Farhad Nemati Taher, Kazem Razmi, Reza Tasouji Azar, Tube bundle replacement for segmental and helical shell and tube heat exchangers: Performance comparison and fouling investigation on the shell side, Applied Thermal Engineering51(2013) 1162e1169
10. Jian-Fei Zhang, Ya-Ling He, Wen-Quan Tao, 3D numerical simulation on shell-and-tube heat exchangers with middle-overlapped helical baffles and continuous baffles – Part I: Numerical model and results of whole heat exchanger with middle-overlapped helical

ISSN: 2277-9655
Scientific Journal Impact Factor: 3.449
(ISRA), Impact Factor: 2.114

baffles, International Journal of Heat and Mass Transfer 52 (2009) 5371–5380

11. Qiuwang Wang, Numerical investigation on combined multiple shell-pass shell-and-tube heat exchanger with continuous helical baffles, International Journal of Heat and Mass Transfer 52 (2009) 1214–122
12. Ya-Ping Chen, Numerical simulation on flow field in circumferential overlap trisection helical baffle heat exchanger, Applied Thermal Engineering 50(2013) 1035e1043
13. B. Peng, Q.W. Wang, C. Zhang, G.N. Xie, L.Q. Luo, Q.Y. Chen, M. Zeng, An experimental study of shell-and-tube heat exchangers with continuous helical baffles, ASME J.Heat Transfer129(2007)1425–1431
14. Jian-Fei Zhang, Ya-Ling He, Wen-Quan Tao, A Design and Rating Method for Shell-and-Tube Heat Exchangers With Helical Baffles, Journal of Heat Transfer, MAY 2010, Vol. 132